A Minimalistic Approach to Segregation in Robot Swarms

Peter Mitrano[1], Jordan Burklund[1], Michael Giancola[1], Carlo Pinciroli[1]

Abstract— We present a decentralized algorithm to achieve segregation into an arbitrary number of groups with swarms of autonomous robots. The distinguishing feature of our approach is in the minimalistic assumptions on which it is based. Specifically, we assume that (i) Each robot is equipped with a ternary sensor capable of detecting the presence of a single nearby robot, and, if that robot is present, whether or not it belongs to the same group as the sensing robot; (ii) The robots move according to a differential drive model; and (iii) The structure of the control system is purely reactive, and it maps directly the sensor readings to the wheel speeds with a simple 'if' statement. We present a thorough analysis of the parameter space that enables this behavior to emerge, along with proofs explaining some of the emergent behavior. Finally, we study the non-ideal aspects in the robot design.

I. Introduction

Group formation is one of the most fundamental mechanisms a robot swarm must exhibit [1]. Group formation can occur in several forms to satisfy different requirements. Segregation is a particular type of group formation in which the focus is on creating local aggregates of robots that share a common property. Segregation can be seen as a precursor to object sorting, task allocation, or self-assembly. For example, swarms may need to split into arbitrary groups to diffuse and search different areas, or segregate by skill or capability in order to form useful heterogeneous teams.

Segregation is an example of the broader class of spatially organizing behaviors, whose purpose is to impose a structure in the environment (e.g., object clustering [2], collective construction [3]) or in the distribution of the robots (e.g., aggregation [4], pattern formation [5], self-assembly [6]).

A recent line of research in spatially organizing behaviors focuses on the *minimal* assumptions a swarm of robots must fulfill in order to perform the task. Johnson and Brown [7] and Brown *et al.* [8] characterized the set of possible behaviors that can be obtained using primordial control strategies based on a simple 'if/then/else' structure, binary sensors, and differential-drive robots. Gauci *et al.* provided the specific conditions for the emergence of aggregation [9] and object clustering [2], while St.-Onge *et al.* [10] studied the emergence of circular formations. While more efficient control strategies have been proposed to achieve these behaviors, studying the minimal assumptions required for their emergence is an important step towards principled 'swarm engineering' practices. In addition, these minimal behaviors might offer last-resort solutions in case of sensor failures

in remote environments such as in planetary exploration missions.

This paper furthers this line of inquiry by studying the minimal assumptions for N-class segregation to emerge from local, decentralized interactions among robots. The term 'N-class' refers to the creation of N spatially distinct groups. We show that, for segregation to emerge, it is sufficient to equip an 'if/then/else', differential drive robot with a *ternary* sensor. This sensor detects the presence of a robot along a line-of-sight. When a robot is detected, the sensor can distinguish whether it is a *kin*, i.e., it belongs to the same group as the sensing robot, or a *non-kin*, i.e., it belongs to a different group. When multiple robots are in range, the sensor returns information on the closest one of them.

The main contributions of this paper are *(i)* A study of the parameter space that enables the emergence of N-class segregation; *(ii)* A study of why certain behavior is guaranteed for the best parameter choice found; and *(iii)* An analysis of the robustness of the algorithm to non-idealities in the robot design.

II. Related Work

Segregation is a common behavior in nature, and it can be observed across scales. For example, cell segregation is a basic building block of embryogeneis in tissue generation processes [11], [12]; while social insects, such as ants, organize their brood into ring-like structures [13].

In robotics, segregation is a problem that has not received considerable attention. The main methods that have been proposed so far are based on some variation of the artificial potential approach [14], which assumes that the robots can detect each other and estimate relative distance vectors.

Groß *et al.* [15] proposed an algorithm inspired by the Brazil Nut effect, in which the robots form regular layers simulating gravity by sharing a common direction. This study was later extended to work on e-pucks robots [16]. To simulate gravity, this approach requires the robots to share a common target vector, which can be obtained through centralized controllers or a distributed consensus algorithm.

Kumar *et al.* [17] introduced the concept of "differential potential", whereby two robots experience a different artificial potential depending on their being part of the same class or not. The convergence of this approach is guaranteed for two classes, but when more classes are employed local minima prevent segregation from emerging.

Santos *et al.* [18] took inspiration from [17] to devise an approach based on the Differential Adhesion Hypothesis,

[1] Robotics Engineering, Worcester Polytechnic Institute, MA, USA. Email: cpinciroli@wpi.edu
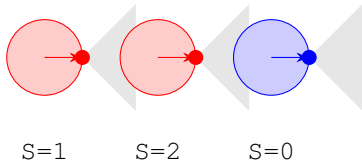
S=1   S=2   S=0

Fig. 1: A diagram of the ternary sensor in which classes are depicted as colors. The left red robot detects a kin robot, so its sensor returns 1. The middle red robot detects a blue robot, so its sensor returns 2. The right robot detects no robot, so its sensor returns 0.

Algorithm 1 The segregation control algorithm.
---
if $S = 0$ **then**
    set wheel speeds to $v_{\text{left}}^{S=0}$, $v_{\text{right}}^{S=0}$
else if $S = 1$ **then**
    set wheel speeds to $v_{\text{left}}^{S=1}$, $v_{\text{right}}^{S=1}$
else
    set wheel speeds to $v_{\text{left}}^{S=2}$, $v_{\text{right}}^{S=2}$
end if

---

which states that kin cells tend to adhere stronger than non-kin cells. However, one limitation is the assumption that the robots have global knowledge about the positions of other robots.

To the best of our knowledge, this paper is the first to propose a segregation algorithm that is not based on global information nor on communication and sensing of multiple neighbors.

III. METHODOLOGY

A. Problem Formulation

Motion model. We consider a set of robots executing the same controller in a two-dimensional, obstacle-free environment. The robots are equipped with two wheels for which $[v_{\text{left}}, v_{\text{right}}]$ denote their *normalized* linear speeds. By 'normalized' we mean that the speed values are in the range $[-1, 1]$. Using normalized speeds allows us to reason in a general way over the specific speeds attainable by any robot. To transform from normalized speeds $[v_{\text{left}}, v_{\text{right}}]$ into actual speeds $[V_{\text{left}}, V_{\text{right}}]$, we introduce a parameter V_{max} that denotes the maximum linear speed possible with a specific robot and define

$$V_{\text{left}} = V_{\text{max}} v_{\text{left}} \tag{1}$$
$$V_{\text{right}} = V_{\text{max}} v_{\text{right}}. \tag{2}$$

The robots' motion assuming constant wheel velocities is modeled by the well-known differential-drive equations, shown in Equation (5).

Sensor model. The robots are also equipped with a ternary sensor that is able to detect the presence of nearby robots and their "kinness". Two robots are *kin* if they belong to the same class (denoted by color in our experiments); they are *non-kin* otherwise. The sensor is assumed to have infinite range (we consider non-infinite range in Sec. VI-D). As depicted in Fig. 1, the sensor returns a reading $S = 0$ when

no robot is detected, $S = 1$ when a kin robot is detected, and $S = 2$ when a non-kin robot is detected. We allow for any number of classes, but the sensor need not distinguish between different non-kin classes—it only detects whether a nearby robot belongs to the same class or not.

Control logic. The control logic followed by the robots is formalized in Alg. 1. It is a simple 'if/then/else' structure, which maps the sensor readings S directly into normalized wheel speeds $[v_{\text{left}} \ v_{\text{right}}]$. The latter are the parameters whose value we intend to study, and they can be encoded as a six-dimensional vector

$$[\, v_{\text{left}}^{S=0} \ v_{\text{right}}^{S=0} \ v_{\text{left}}^{S=1} \ v_{\text{right}}^{S=1} \ v_{\text{left}}^{S=2} \ v_{\text{right}}^{S=2} \,].$$

Objective. The objective of our study is to find the values of the speed parameters for which the robots group into clusters, such that all the robots of the same class are packed into one cluster with no non-kin robots.

B. Simulation Environment and Robots

Simulation platform. We utilized the ARGoS multi-robot simulator [19] to search for controller parameters and evaluate them. ARGoS offers accurate models for several differential-drive robots, such as the foot-bot [20], the Khepera IV[1], and the Kilobot [21].

Simulated Robot platform. For the simulated experiments we opted to use the foot-bot, because of the possibility to utilize its range-and-bearing communication system as a base for the ternary sensor. The advantage of using the range-and-bearing system is that its model is simple and, as a consequence, a large number of simulations could be completed in a short time. The range-and-bearing system allows two robots to exchange messages when they are in direct line-of-sight; upon receiving a message, a robot can also estimate the relative position of the sender. This sensor, in principle, receives messages from all the nearby robots. To simulate the ternary sensor, our robot controller kept the message of the closest robot. The message payload was an integer that encoded the id of the group to which the sender belonged. The range-and-bearing sensor is simulated through ray casting. This allowed us to assume that the sensor reading is infinitely thin, a choice that simplifies the mathematical analysis presented in Sec. V. However, in practical applications, the sensor can be expected to cast a cone-shaped sensory range with non-zero aperture angle. We explore the performance effect of various angles in Sec. VI-C.

C. Grid Search

Trial setup. In order to exhaustively search the space of possible controllers, we conducted a grid search of the 6-dimensional parameter space. Due to limited computational resources, we were only able to search with a resolution of 7 values per parameter: $[-1, -\sfrac{2}{3}, -\sfrac{1}{3}, 0, \sfrac{1}{3}, \sfrac{2}{3}, 1]$. In total we evaluated $7^6 = 117,649$ parameter sets. For each parameter set, we tested 36 different initial configurations

---
[1]https://www.k-team.com/khepera-iv

(8 with 1-class, 8 with 2-class, 20 with 4-class), with 100 simulated seconds for each trial. These initial configurations consisted of uniformly random placement, clusters, and lines of robots distributed throughout the environment. We chose to include some structured configurations (clusters and lines) because we discovered that they affected significantly the performance with respect to uniform random configurations. Hence, by explicitly evaluating diverse initial configurations, we could better estimate the best parameter values in the general case. Examples of these starting configurations can be seen in our supplementary videos [2].

Clusters. To define our cost function, we first establish the notion of a cluster. A cluster can be intuitively defined as an island of connected kin robots. Formally, a cluster is a set of kin robots which are *connected*. Denoting with r the radius of the body of a robot, and defining $\mathbf{p}_i(t) = [x_i(t)\ y_i(t)]$ as the x and y coordinates of the robot i at time t, we consider any two kin robots to be connected if

$$\|\mathbf{p}_i(t) - \mathbf{p}_j(t)\| \leq 2r + \epsilon \qquad (i \neq j, \epsilon \in \mathbb{R}^+) \quad (3)$$

In our experiments, we set $\epsilon = 5\,\mathrm{cm}$. We find clusters by first constructing an adjacency matrix and then performing a depth-first search. Since we are interested in segregating the robots in N classes, the final result of a trial is expected to be a set of N distinct clusters composed of kin robots.

Cost function. To measure the difference between the ideal, perfectly segregated result and any configuration achieved by the robots over time, we first calculate, for every class i, the number of robots in the largest cluster $c_i(t)$ formed by robots of class i. Since, in principle, different classes might involve different numbers of robots, in our cost function we employ the ratio

$$\gamma_i(t) = -\frac{c_i(t)}{C_i}$$

This ratio should be maximized, so the negative sign assigns larger clusters a lower, more negative, cost. Here C_i is the number of robots that belongs to class i. At each time step, the cost is

$$\gamma(t) = \frac{1}{N} \sum_{i=1}^{N} \gamma_i(t)$$

Our complete cost function is then

$$c_{\text{total}} = \sum_{t=0}^{T-1} t\gamma(t) \quad (4)$$

in which we denote the total trial time (100 seconds) with T. The effect of multiplying $\gamma_i(t)$ by t is to highlight the emergence of clusters as the trial time proceeds: we cannot expect large clusters to be present at the beginning of a trial, but good parameter settings should grow (and maintain) clusters over time. In our experiments, we found from visual inspection that c_{total} correctly assigns cost in most scenarios. However, this cost function considers a straight line of robots to be a cluster, and as such it might not be ideal for scenarios in which the clusters are required to be tight.
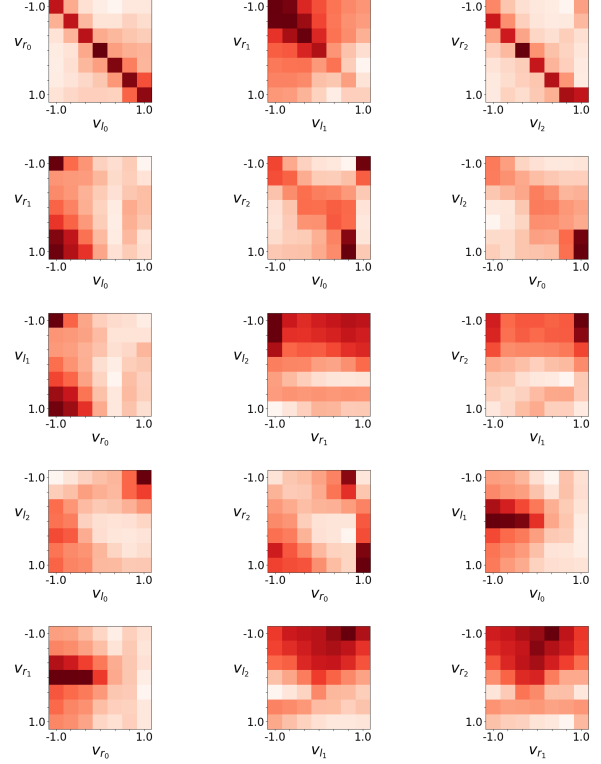
Fig. 2: Heatmaps that relate relevant pairs of wheel speeds. Darker is worse.

IV. THE EMERGENT BEHAVIOR

Visualizing grid search. The results of grid search are reported in Fig. 2. Because the search space is six-dimensional, we chose to visualize it by plotting every pair of parameters against each other. For example, we consider how the cost changes as $v_{\text{left}}^{S=0}$ and $v_{\text{right}}^{S=0}$ change. As an example of reading these plots, we can tell from the plot of $v_{\text{left}}^{S=1}$ and $v_{\text{right}}^{S=1}$ that there were no good controllers where the left and right wheel speeds were equal and negative (dark squares in the upper left), and that the best controllers had unequal values close to 1 (lightest squares in the bottom left). These plots also convey the presence of sharp discontinuities where performance changes dramatically.

The emergent behavior. After running the grid search, the parameters with the lowest mean cost across all 36 starting configurations

$$[-1, 1/3, 1/3, 1, -1, 1]. \quad (C)$$

The resulting behavior is for a robot to turn sharply until it detects a kin, then turn less sharply while it sees the kin. This change in the radius of rotation moves the robot closer to its kin. When a non-kin is seen, the robot turns in place. In isolation, the emergent behavior between kin and non-kin is similar to the aggregation behavior found by Gauci *et al.* [9] in that the robots are always turning in the same direction (counter-clockwise for our parameters). To our surprise, we found that the best segregation behavior requires that non-kin also aggregate. This was not only

true for the best parameters, but for all of the top-scoring parameters we observed. To better appreciate the dynamics of this behavior, we invite the interested reader to watch the videos at https://goo.gl/z8UAuB.

V. Behavior Analysis

Using the parameter settings (C), we now break down and analyze the emerging behavior. While we are not able to formally explain the segregation behavior among an arbitrary number of robots, we can instead consider simplified scenarios with two robots. We prove that, for the robot parameters considered in our experiments, two kin robots in isolation are guaranteed to aggregate. Interestingly, we also show that two isolated non-kin robots are also guaranteed to aggregate. We hypothesize that this aggregation of non-kin is actually useful for segregation with this sensor model, since by keeping robots close we ensure that kin robots are not initially repelled by non-kin and fail to discover each other. This is supported by our grid search results, for which we found that the vast majority of the top scoring parameters showed aggregation between isolated non-kin. These two guarantees partially explains the emergent behavior observed in our experiments.

In the proofs, we employ the well-known equations that govern the instantaneous radius of curvature R and rotation speed ω of the path followed a differential-drive robot with l denoting the interwheel distance [22]:

$$
\begin{aligned}
R &= \frac{l}{2}\frac{V_{\text{right}} + V_{\text{left}}}{V_{\text{right}} - V_{\text{left}}} = \frac{l}{2}\frac{v_{\text{right}} + v_{\text{left}}}{v_{\text{right}} - v_{\text{left}}} \\
\omega &= \frac{V_{\text{right}} - V_{\text{left}}}{l} = \frac{V_{\text{max}}(v_{\text{right}} - v_{\text{left}})}{l}.
\end{aligned}
\tag{5}
$$

Table I shows values of R and ω for each sensor value, which we then use in our proofs.

We simplify the geometry by assuming that the sensor is an infinitely thin beam, that both robots are synchronized such that they take sensor readings at the same time, and that both robots act for the same $\Delta t = 0.1$ time step. Lastly, we assume the robots a radius of $r = 0.085$, interwheel distance $l = 0.14$, and scaling velocity V_{max}.

We consider all of the possible sensor values ($S = 0$, $S = 1$, $S = 2$) for a robot i and a second robot j in separate cases. However, the cases ($S_i = 1$, $S_j = 0$) and ($S_i = 0$, $S_j = 1$) and the cases ($S_i = 2$, $S_j = 0$) and ($S_i = 0$, $S_j = 2$) are equivalent so we need only prove aggregation for one of each pair. Furthermore, for two isolated robots, the cases where one robot sees a kin and the other sees a non-kin ($S_i = 1$, $S_j = 2$) and ($S_i = 1$, $S_j = 2$) are impossible.

	$S = 0$	$S = 1$	$S = 2$
v_l	-1	$1/3$	-1
v_r	$1/3$	1	1
R	$-l/4$	l	0
ω	$\frac{4V}{3l}$	$\frac{2V}{3l}$	$\frac{2V}{l}$

TABLE I: turning Radii and rotational velocities for the best parameters.

This leaves just 5 cases, and in each case we prove that the robots aggregate.

We use x, y, and α, collectively called a configuration, to indicate the location of robot j relative to robot i. Without loss of generality, we will always consider robot i to be at the origin and facing the positive x-axis. Rather than showing that the center point of the robots p_i and p_j aggregate, we show that the points c_i and c_j aggregate. These are the points around which the robot rotates in the $S = 0$ case. These points are at a distance $\frac{l}{4}$ from the center of the robot, and therefore when $c_i = c_j$ the points p_i and p_i are at most $\frac{l}{2}$ apart. On a real robot, the half of the inner wheel distance l must be less than the robot radius r (or the wheels would protrude from the robot). Hence aggregation of c_i and c_j is equivalent to the aggregation of p_i and p_j.

As discussed above, there are 5 sensor cases to be considered for two robots. In the "see nothing" case ($S_i = 0$, $S_j = 0$), we will prove that the points c_i and c_j remain at constant distance. We then prove that in the other 4 cases the points aggregate. Finally, if c_i and c_j are guaranteed to exit the "see nothing" case into one of the other four sensor cases where they aggregate, then they must eventually aggregate regardless of when and how often they may transition between the different sensor cases.

Theorem 1 (Nothing Detected): In the sensor case ($S_i = 0$, $S_j = 0$), the robots will transition to another sensor case if

$$
||p_j - p_i|| \lessgtr 0.888\text{m}
\tag{6}
$$

Proof: In this sensor case the robots rotate around the points c_i and c_j, and therefore these points are stationary. To prove that c_i and c_j eventually aggregate we must prove that the robots exit this sensor case. In other words, we prove that one robot will eventually see the other. For this, the distance between the robots must be bounded. If the robots are too far away, then the beam could "skip" over the other robot. Furthermore, we account for the fact that robot j is also moving. Figure 3 shows the robots in the configuration where this maximum distance is attained. In this worst-case configuration, the bottom of robot j is tangent to the beam of robot i at $t = 0$. Then at $t = 0.1$, the top of robot j is tangent to the new beam of robot i. Since we know the angles the robots rotate, this fully constraints the geometry to the configuration shown. We used the Geometry package Geogebra [23] to solve for the bound in this equation. ■

Theorem 2 (Kin Robots #1): In the case ($S_i = 1$, $S_j = 0$), the robots aggregate.

Proof:

Robot j is in state $S = 0$, rotating around the point c_j. Therefore c_j is stationary, so we require $||c_j - c_i'|| < ||c_j - c_i||$. We draw the perpendicular bisector between c_i and c_i' (thick black line, Figures 4a, 4b) and note that c_j is always on the left side of this line, and therefore $||c_j - c_i'|| < ||c_j - c_i||$ holds. ■

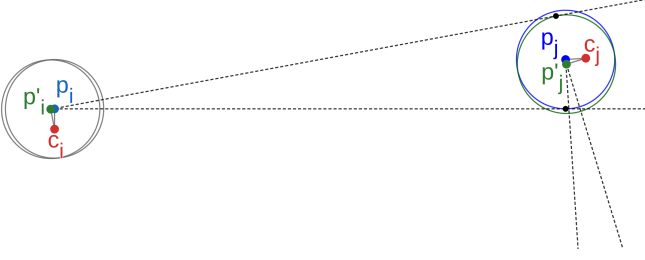*Theorem 3 (Non-Kin Robots #1):* In the case ($S_i = 2$, $S_j = 0$), the robots aggregate.

Proof:

Fig. 3: Two robots at the maximum distance at which the robots will not skip over seeing each other. Robot i moves from p_i to p_i', and likewise for robot j. Without loss of generality, we place p_i at the origin initially facing the positive x-axis. Figure is accurate up to a scale.

This proof follows the reasoning from Theorem 2, and is illustrated in Figure 4b. ∎

Theorem 4 (Kin Robots #2): In the case ($S_i = 1$, $S_j = 1$), the robots aggregate.

Proof:

As in the previous proofs, the region of possible configurations (x, y, α) of robot j is bounded for this sensor case. This range for x is bounded on the left by collision with the kin and on the right by a distance $0.888\,\mathrm{m}$. In y, the range is bounded by $-r$ and r because in this case we require robot i to see robot j. Finally, the α value is bounded by $120°$ and $240°$ because in this sensor case robot j sees robot i. This minimum and maximum α are shown in Figure 6. We then numerically check exhaustively over this space with a fine resolution, shown in Figure 5a. ∎

Theorem 5 (Non-Kin Robots #3): In the case ($S_i = 2$, $S_j = 2$), the robots aggregate.

Proof:

This proof follows the reasoning from Theorem 4, and is illustrated in Figure 5b. ∎

VI. EXPERIMENTAL RESULTS

A. Scalability Study

In this experiment we investigate how the segregation behavior scales with the number of classes and the number of robots in the environment. We varied the number of classes from 1 to 25 and ran 100 trials with robots uniformly randomly distributed. All trials lasted 180 seconds.

Fixed number of robots per class. We studied the case in which every class has 10 robots. The results of this are plotted in Fig. 7. We observe that the cost increases with the number of classes. As the number of classes increases, the density of the robots increases too. Hence, line-of-sight occlusions between robots are more likely, navigation is more difficult, and the clusters do not have a chance to coalesce. The important trend is that as the number of robots increases, the cost increase sublinearly. This suggests that our method scales well with the total number of robots.
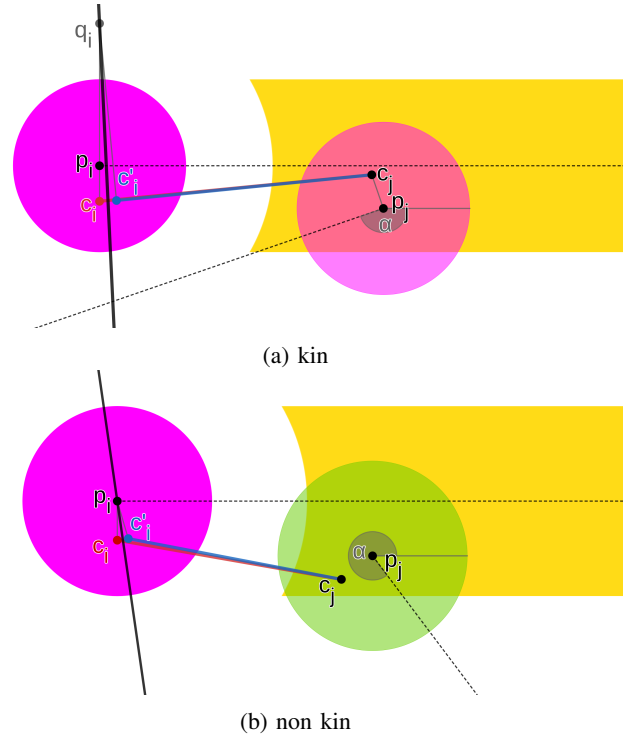

(a) kin

(b) non kin

Fig. 4: Robot i sees robot j and robot j sees nothing. c_i moves to c_i' and is closer to c_j. The point p_x must be in the yellow region (which extends past the right of this image up to $0.888\,\mathrm{m}$, and α is such that the beam of robot j must not intersect robot i. The dashed lines represent the sensor beams. In this figure, one example p_j and α is shown.

Fixed total number of robots. We considered the scenario in which a fixed number of robots is split into an increasing number of classes. We set the number of robots to 100, so with 25 classes 4 robots were still assigned to each class. As reported in Fig. 8, the cost is very low for small numbers of classes and above 5 classes has no trend in cost. The initial low cost is due to the fact that with 100 robots to divided among few classes, line-of-sight to a kin is highly likely. Here the trend indicates that our methods scaled well with the number of classes.

B. The Effect of Implementation Details of the Sensor

We observed that the implementation details of the sensor have a significant effect on the behavior of the controller.

Initially, our method for determining sensor value from the simulated range-and-bearing system was to consider all the robots within some small angle in front of the robot and pick the closest one. This is very similar to what would be provided by a real-world camera that uses colored skirts on each robot and picks the largest blob as the robot to be detected. This sensor implementation works well and was used in all our experiments. However, we found later that, if the robots instead always prefer to react to kin over non-kin, clusters form more quickly and robustly. For example, if there are two robots within the field of view of a robot's sensor and the non-kin robot is closer, the robot would ignore
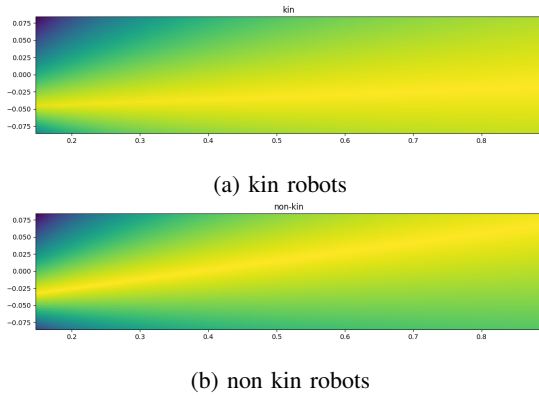
(a) kin robots

(b) non kin robots

Fig. 5: A numerical check visualizing how much closer the two robots are after one time step. All values are positive because aggregation occurs everywhere, yellow means more aggregation. The dashed lines represent the sensor beams.
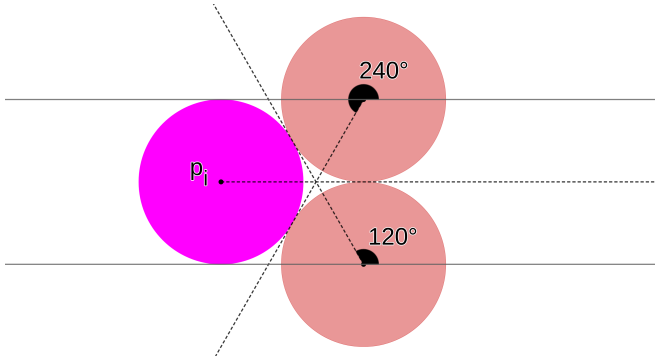

Fig. 6: Visualization of the minimum and maximum value for α for the sensor cases ($S_i = 1$, $S_j = 1$) and ($S_i = 2$, $S_j = 2$).

it and execute the $S = 1$ logic, which drives the robot towards the farther kin robot. Exploring exactly which of the various implementation details have what effect on cost is left for future work.

C. The Effect of the Beam Angle

On a real robot, there must be some finite beam angle to the theoretically line-of-sight sensor. We ran 100 trials 180 seconds each in simulation with uniformly random initial distributions of 40 robots with various beam angles. Fig. 9 shows the results, along with a diagram showing how we define beam angle. The best beam angle we tested was $20°$, and angles smaller or larger became progressively worse. We found that at lower beam angles, it was possible for a robot to become stuck in groups of two or three, and the robots spent all their time looking at each other instead of peeking around them to find kin. At larger angles, we suspect the behavior fails because larger beam angles cause the rings to enlarge faster. When the rings become too large and the space between robots exceeds $2r + \epsilon$ and are no longer a cluster as defined by (3).
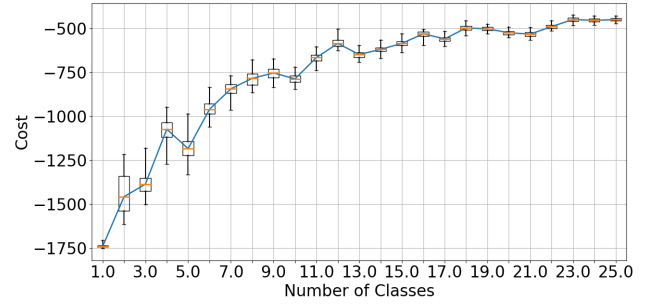

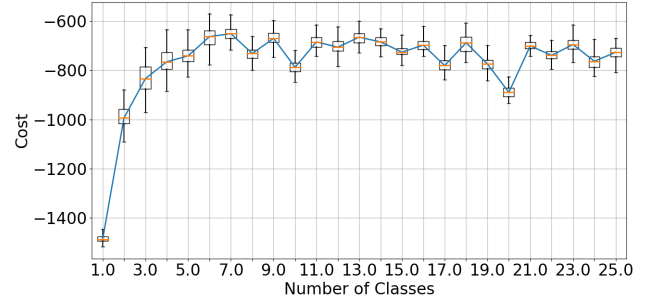Fig. 7: The average cost over 100 trials with N classes, 10 robots per class.

Fig. 8: The average cost over 100 trials with 100 robots divided into N classes.

D. The Effect of Beam Length

We consider what happens if the theoretically infinite-range sensor has finite range. We use $15°$ half beam angle and the same experimental setup as with the beam angle experiments. We consider the maximum range of the sensor as the diagonal length of the square in which the robot are initially distributed. In all our experiments, this square was $5\,\mathrm{m}$ on each side, so we consider a range of $7.07\,\mathrm{m}$ to be effectively unlimited. We report the costs for beam ranges as a fraction of this maximum range. As shown in Fig. 10, a beam range of 25% of the theoretical maximum performs just as well as an infinite sensor. Below this, the performance degrades.

VII. Conclusion

In this paper, we show how robots with only a ternary sensor and a controller which maps sensor readings to wheel speeds is capable of N-class segregation. This controller is invariant to the number of classes, and using the best found parameters we are able to construct theoretical guarantees on the emergent behavior in a simplified setting. We performed a grid search to learn about the full parameter space, and we investigated the effect of sensor implementation details and the number of robots and classes on performance. Our findings indicate that robust segregation with non-ideal sensors in reality is possible, although not guaranteed.
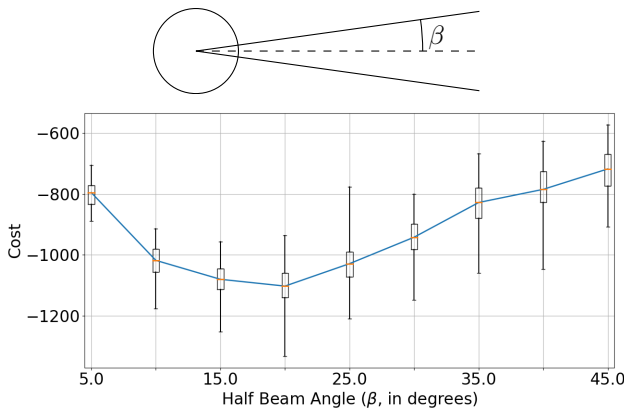
Fig. 9: A 15° degree half beam angle is best for segregation. Lower cost is better.
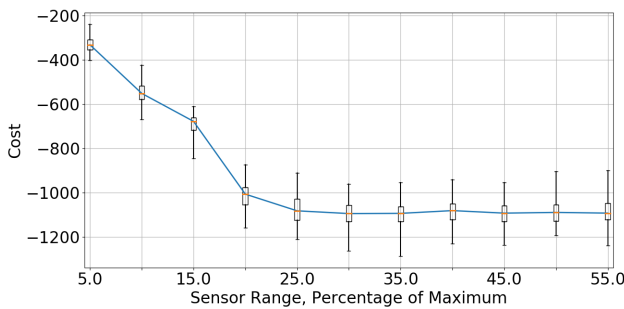

Fig. 10: Segregation is robust to small sensor beam ranges. The performance at 25% of maximum range is indistinguishable from infinite range.

REFERENCES

[1] M. Brambilla, E. Ferrante, M. Birattari, and M. Dorigo, "Swarm robotics: A review from the swarm engineering perspective," *Swarm Intelligence*, vol. 7, no. 1, pp. 1–41, 2013.

[2] M. Gauci, J. Chen, W. Li, T. J. Dodd, and R. Groß "Clustering Objects with Robots That Do Not Compute," in *Proceedings of the 2014 International Conference on Autonomous Agents and Multi-agent Systems*, ser. AAMAS '14. Richland, SC: International Foundation for Autonomous Agents and Multiagent Systems, 2014, pp. 421–428. [Online]. Available: http://dl.acm.org/citation.cfm?id=2615731.2615800

[3] A. Bolger, M. Faulkner, D. Stein, L. White, and D. Rus, "Experiments in decentralized robot construction with tool delivery and assembly robots," in *2010 IEEE/RSJ Int. Conf. on Intelligent Robots and Systems (IROS 2010)*. IEEE Press, 2010, pp. 5085–5092.

[4] N. E. Shlyakhov, I. V. Vatamaniuk, and A. L. Ronzhin, "Survey of Methods and Algorithms of Robot Swarm Aggregation," *Journal of Physics: Conference Series*, vol. 803, p. 012146, Jan. 2017. [Online]. Available: http://stacks.iop.org/1742-6596/803/i=1/a=012146?key=crossref.a3ceb0f2b8113f73c39aa6e56ddeeb8a

[5] C. Pinciroli, A. Gasparri, E. Garone, and G. Beltrame, "Decentralized progressive shape formation with robot swarms," in *13th International Symposium on Distributed Autonomous Robotic Systems (DARS2016)*, ser. Springer Proceedings in Advanced Robotics. Springer, November 2016, pp. 433–445.

[6] R. Groß and M. Dorigo, "Self-assembly at the macroscopic scale," *Proceedings of the IEEE*, vol. 96, no. 9, pp. 1490–1508, 2008.

[7] M. Johnson and D. Brown, "Evolving and Controlling Perimeter, Rendezvous, and Foraging Behaviors in a Computation-Free Robot Swarm," in *Proceedings of the 9th EAI International Conference on Bio-inspired Information and Communications Technologies (Formerly BIONETICS)*, ser. BICT'15. ICST, Brussels, Belgium,

Belgium: ICST (Institute for Computer Sciences, Social-Informatics and Telecommunications Engineering), 2016, pp. 311–314. [Online]. Available: http://dx.doi.org/10.4108/eai.3-12-2015.2262390

[8] D. S. Brown, R. Turner, O. Hennigh, and S. Loscalzo, "Discovery and Exploration of Novel Swarm Behaviors Given Limited Robot Capabilities," in *Distributed Autonomous Robotic Systems*, ser. Springer Proceedings in Advanced Robotics. Springer, Cham, 2018, pp. 447–460. [Online]. Available: https://link.springer.com.ezproxy.wpi.edu/chapter/10.1007/978-3-319-73008-0_31

[9] M. Gauci, J. Chen, T. J. Dodd, and R. Groß "Evolving Aggregation Behaviors in Multi-Robot Systems with Binary Sensors," in *Distributed Autonomous Robotic Systems*, ser. Springer Tracts in Advanced Robotics. Springer, Berlin, Heidelberg, 2014, pp. 355–367. [Online]. Available: https://link.springer.com/chapter/10.1007/978-3-642-55146-8_25

[10] D. St-Onge, C. Pinciroli, and G. Beltrame, "Circle formation with computation-free robots shows emergent behavioral structure," in *Proceedings of the IEEE/RSJ International Conference on Intelligent Robots and Systems (IROS 2018)*. Madrid, Spain: IEEE Press, October 2018, in press.

[11] E. Batlle and D. G. Wilkinson, "Molecular Mechanisms of Cell Segregation and Boundary Formation in Development and Tumorigenesis," *Cold Spring Harbor Perspectives in Biology*, vol. 4, no. 1, p. a008227, Jan. 2012. [Online]. Available: http://cshperspectives.cshlp.org/content/4/1/a008227

[12] M. S. Steinberg, "Reconstruction of tissues by dissociated cells," *Science*, vol. 141, pp. 401–408, 1963.

[13] N. N. Franks and A. Sendova-Franks, "Brood sorting by ants: distributing the workload over the work-surface," *Behavioral Ecology and Sociobiology*, vol. 30, no. 2, pp. 109–123, 1992.

[14] W. M. Spears, D. F. Spears, J. C. Hamann, and R. Heil, "Distributed, Physics-Based Control of Swarms of Vehicles," *Autonomous Robots*, vol. 17, no. 2/3, pp. 137–162, Sep. 2004.

[15] R. Groß S. Magnenat, and F. Mondada, "Segregation in swarms of mobile robots based on the Brazil nut effect," in *2009 IEEE/RSJ International Conference on Intelligent Robots and Systems*, Oct. 2009, pp. 4349–4356.

[16] J. Chen, M. Gauci, M. J. Price, and G. R, "Segregation in swarms of e-puck robots based on the brazil nut effect," in *Proc. of the 11th Int. Conf. on Auton. Agents and Multi-agent Syst.*, 2012, pp. 163–170.

[17] M. Kumar, D. P. Garg, and V. Kumar, "Segregation of Heterogeneous Units in a Swarm of Robotic Agents," *IEEE Transactions on Automatic Control*, vol. 55, no. 3, pp. 743–748, Mar. 2010.

[18] V. G. Santos, L. C. A. Pimenta, and L. Chaimowicz, "Segregation of multiple heterogeneous units in a robotic swarm," in *2014 IEEE International Conference on Robotics and Automation (ICRA)*, May 2014, pp. 1112–1117.

[19] C. Pinciroli, V. Trianni, R. O'Grady, G. Pini, A. Brutschy, M. Brambilla, N. Mathews, E. Ferrante, G. D. Caro, F. Ducatelle, M. Birattari, L. M. Gambardella, and M. Dorigo, "ARGoS: a Modular, Parallel, Multi-Engine Simulator for Multi-Robot Systems," *Swarm Intelligence*, vol. 6, no. 4, pp. 271–295, 2012.

[20] M. Bonani, V. Longchamp, S. Magnenat, P. Rétornaz, D. Burnier, G. Roulet, F. Vaussard, H. Bleuler, and F. Mondada, "The marXbot, a miniature mobile robot opening new perspectives for the collective-robotic research," in *Proceedings of the IEEE/RSJ International Conference on Intelligent Robots and Systems (IROS)*. Piscataway, NJ: IEEE Press, 2010, pp. 4187–4193.

[21] M. Rubenstein, C. Ahler, and R. Nagpal, "Kilobot: A low cost scalable robot system for collective behaviors," *2012 IEEE International Conference on Robotics and Automation*, pp. 3293–3298, May 2012.

[22] G. Dudek and M. Jenkin, *Computational Principles of Mobile Robotics*, 2nd ed. Cambridge University Press, 2010.

[23] M. Hohenwarter, M. Borcherds, G. Ancsin, B. Bencze, M. Blossier, J. Éliás, K. Frank, L. Gál, A. Hofstätter, F. Jordan, Z. Konečný, Z. Kovács, E. Lettner, S. Lizelfelner, B. Parisse, C. Solyom-Gecse, C. Stadlbauer, and M. Tomaschko. (2018, Oct.) GeoGebra 5.0.507.0. http://www.geogebra.org.